PROCEEDINGS OF SCIENCE

Study of the diffuse gamma ray emission from the Galactic plane with ARGO-YBJ

L. L. Ma[1*], B. D'Ettorre Piazzoli[2,3], T. Di Girolamo[2,3] for the ARGO-YBJ Collaboration

1 Key Laboratory of Particle Astrophysics, Institute of High Energy Physics, Chinese Academy of Sciences, P.O. Box 918, 100049 Beijing, P.R. China.
2 Dipartimento di Fisica dell'Università di Napoli "Federico II", Complesso Universitario di Monte Sant'Angelo, via Cinthia, 80126 Napoli, Italy.
3 Istituto Nazionale di Fisica Nucleare, Sezione di Napoli, Complesso Universitario di Monte Sant'Angelo, via Cinthia, 80126 Napoli, Italy.
E-mail: llma@ihep.ac.cn

The data recorded by ARGO-YBJ in more than 5 years have been analyzed to determine the diffuse gamma ray emission from the Galactic plane. The spatial distribution of the diffuse gamma rays and their energy spectra at Galactic longitudes $25^\circ < l < 100^\circ$ and Galactic latitudes $|b| < 5^\circ$ have been studied. The study has been focused on the regions $40^\circ < l < 100^\circ$ and $65^\circ < l < 85^\circ$, where Milagro observed an excess with respect to the predictions of current models. The energy range investigated runs from 350 GeV to 2 TeV, connecting the region explored by Fermi-LAT with the multi-TeV energies studied by Milagro. Great care has been taken in masking the TeV point sources observed by ARGO-YBJ and other experiments. Our results are consistent with the predictions of the Fermi model and do not show any excess as observed by Milagro. From the measured energy distribution spectral indices and differential fluxes at 1 TeV are derived.

The 34th International Cosmic Ray Conference,
30 July- 6 August, 2015
The Hague, The Netherlands

*Speaker.

PoS(ICRC2015)819

1. Introduction

The diffuse gamma-rays from the Galactic plane are produced in processes as the interaction of cosmic nuclei with the interstellar gas through the production and decay of secondary π° mesons, the bremsstrahlung of high energy cosmic electrons and their inverse Compton scattering on low-energy interstellar radiation fields. The spectrum of the diffuse gamma-rays can provide insight into the propagation and confinement in the Galaxy of the parent cosmic rays, their source distribution and their energy spectrum at source. The knowledge of the diffuse gamma-rays is necessary for the accurate detection of gamma-ray sources. In addition, high-quality data on diffuse gamma-rays in the Galactic center region are needed to constrain the dark matter models[1].

At low energies, from 100 MeV to a few GeV, the Galactic diffuse gamma-rays were first detected by the space-born detectors SAS-2[2] and COS-B[3], which revealed the noticeable correlation between the flux of gamma-rays and the density of the interstellar medium. Then COMPTEL and EGRET provided the first maps of diffuse gamma-rays with energy from 1 MeV to 10 GeV[4][5]. In the GeV range, a significant excess was observed in the EGRET data with respect to the predictions based on the cosmic ray flux observed at Earth. However, the excess has not been confirmed by the Fermi-LAT[6] with a sensitivity more than one order of magnitude better than EGRET[7].

At higher energy, due to their low fluxes, the diffuse gamma-rays can be efficiently detected only by ground-based detectors that have large effective areas. The Imaging Atmospheric Cherenkov Telescopes (IACT) H.E.S.S. has carried out the survey of Galactic plane covering the region $-75^{\circ} < l < 60^{\circ}$ in Galactic longitude at an energy threshold of about 250 GeV, and has presented the latitude profile of diffuse gamma-rays with $|b| < 2^{\circ}$[8]. The spatial correlation of gamma-rays with the giant molecular clouds in the inner Galaxy has been also studied, the hardness of gamma-ray spectrum favouring their hadronic origin[9]. However, limited by their field of view (FOV), the IACTs are not well suited to observe the large-scale structure of diffuse gamma-rays.

Air shower arrays providing a large FOV and a very high duty cycle are more adequate for sky survey purposes. The Milagro detector made the first positive observation of diffuse gamma-rays above 3.5 TeV from the Galactic plane in the region $40^{\circ} < l < 100^{\circ}$ and $|b| < 5^{\circ}$ [10]. In a following analysis, Milagro reported a clear excess of diffuse gamma-rays at 15 TeV median energy in the region $65^{\circ} < l < 85^{\circ}$[11]. The Milagro measurements are higher than the fluxes expected from the conventional model. The "TeV excess" may be connected with the "GeV excess" observed by EGRET[12]. However, the Fermi-LAT data do not confirm the excess in the GeV range. Instead, an extended source at $79^{\circ}.6 \pm 0^{\circ}.3$ called "Cygnus cocoon" has been found[13], and its TeV counterpart has been recently identified by the ARGO-YBJ experiment[14]. To better clarify the interpretation of these results, the data collected by ARGO-YBJ were used to study the diffuse gamma-rays in the $25^{\circ} < l < 100^{\circ}$, $|b| < 5^{\circ}$ region.

2. The ARGO-YBJ experiment

The ARGO-YBJ detector, hosted in a building at the YangBaJing Cosmic Ray Observatory (Tibet, China, 90°31'50" E, 30°06'38" N),4300 m above sea level, has been designed for Very High Energy (VHE) gamma-ray astronomy and cosmic ray observations. It is made up of a single

layer of Resistive Plate Chambers (RPCs) operated in streamer mode, 2.850 m $\times$ 1.225 m each, organized in a modular configuration to cover a surface of about 5600 m^2 with an active area of about 93%[15]. More chambers are deployed around this central carpet up to an area of 100 m $\times$ 110 m. A trigger is obtained when at least 20 pads in the central carpet are fired in a time window of 420 ns, which corresponds to an energy threshold of 300 GeV with an effective area depending on the zenith angle. More details about the detector, the RPC performance and the off-line calibrations can be found in [16][17][18][19].

The event reconstruction follows a standard procedure allowing a detailed space time reconstruction of the shower front. The reconstruction algorithms can be found in [20] [21] [22][23]. The angular resolution depends on the number of fired pads N_{pad}. The opening angle ψ_{70} containing 71.5% of the events from a point source is about 2° for $N_{pad} > 20$, 1.36° for $N_{pad} > 60$ and 0.99° for $N_{pad} > 100$. The number of hit pads N_{pad} is related to the primary energy. However, it is not a very accurate estimator of the primary energy due to the large fluctuations in the shower development and to its partial sampling with the limited detector area. The relation between N_{pad} and energy can be found in [23]. The angular resolution, pointing accuracy, absolute energy calibration and detector stability are tested by measuring the Moon shadow[21].

3. Data analysis

The ARGO-YBJ has been operated stably for 5.3 yr, with an average duty cycle of 86%, for a total effective time of 1670.45 days. For the present analysis, events with zenith angles less than 50°, and $N_{pad} > 20$ are used. A set of standard cuts, applied to the reconstructed shower core and to the time spread of the shower front, have been used to select high-quality data. With these data selections, the fraction of survived events is about 80%, and more background cosmic rays than gamma-rays are rejected, with a corresponding increase of the sensitivity[22]. The selected data are used to study the diffuse gamma-rays from the Galactic plane regions $25^\circ < l < 100^\circ$ and $130^\circ < l < 200^\circ$. The region $100^\circ < l < 130^\circ$ is excluded since in the high declination region the Galactic plane is parallel the right ascension axis, and the contribution from the signal could affect the background estimation. All the events are divided into 3 pad groups, $20 < N_{pad} \leq 59$, $60 \leq N_{pad} \leq 99$ and $N_{pad} \geq 100$ and fill, for each group, a grid of $0.1^\circ \times 0.1^\circ$ bins according to their reconstructed directions. The background of cosmic-ray is estimated by the direct integration method[24]. Then the excess map is obtained by subtracting the background map to the event map.

The effect of cosmic ray anisotropy on the background evaluation has been estimated and corrected by applying the normalization given in [20]. This procedure is applied to each map bin using a surrounding region of $16^\circ \times 16^\circ$ in which the estimated background is renormalized to the detected events. The $\pm 5^\circ$ region around the Galactic plane and the $4^\circ \times 4^\circ / cos(b)$ region around the Crab Nebula position are excluded from the normalization procedure. However, since the diffuse gamma-ray emission extends to more than $|b| = 5^\circ$, its contribution causes an overestimation of the correction related to the cosmic ray anisotropy. This effect has been evaluated using the latitude profile provided by the Fermi-LAT model for the diffuse Galactic emission smeared out with the ARGO-YBJ Point Spread Function (PSF). The box size has been varied from $12^\circ \times 12^\circ$ to $20^\circ \times 20^\circ$ to study the systematic errors, obtaining an excess variation of about 10%.

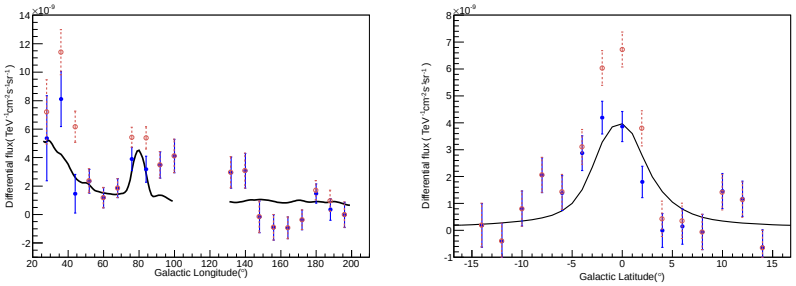

Figure 1: left:Galactic longitude profile of the diffuse gamma-rays in the latitude belt $|b| < 5^\circ$. right: Galactic latitude profile of the diffuse gamma-rays in the longitude belt $25^\circ < l < 100^\circ$. The fluxes are given at 600 GeV. The filled circles show the results after masking the sources, while the open circles show the results without the masking. The solid line represents the value quoted by the Fermi-DGE model at the same energy, smeared out with the ARGO-YBJ PSF.

Many TeV sources have been detected in the Galactic plane. Source locations as given in the TeVCat[1] are excluded. Considering the angular resolution of the detector and the extension of the sources, the contribution from a region $4^\circ \times 4^\circ/cos(b)$ centered at the source location is removed. Sources distant less than $1^\circ.2$, as for instance HESS J1857+026 and HESS J1858+020, have been masked with a unique box centered at the median point. Since the extension of the Fermi Cocoon is about 2°[13], this region has been masked with a box $6^\circ \times 6^\circ/cos(b)$ centered on the position found by ARGO-YBJ[14]. The chosen dimension of these boxes is a compromise between a desired large excluded region, in order to minimize the contamination from the sources, and the requirement of not reducing the statistics. With this choice the solid angle of the region $25^\circ < l < 100^\circ$, $|b| < 5^\circ$ is reduced of about 22%. The contribution of the sources outside the masked regions is estimated by tracking their path inside the ARGO-YBJ FOV. The contamination is calculated bin by bin and subtracted from the event excess map. For ARGO J1839-0627/HESS J1841-055, ARGO J1907+0627/MGRO J1908+06 and ARGO J2031+4157 (the Cygnus cocoon) the fluxes measured by ARGO-YBJ have been considered[22][14]. Since the PSF broadens with decreasing energy, this contamination is found higher for the first energy bin , with an average value of 14%, while it is 21% in the Cygnus region $65^\circ < l < 85^\circ$.

4. Results

The Galactic longitude profile of the diffuse gamma-rays at 600 GeV in the latitude belt $|b| < 5^\circ$ is shown in the left plot of Fig. 1 by filled circles, representing the fluxes obtained with the spectral analysis. The flux of all the events with $N_{pad} > 20$ is calculated by using the effective areas estimated by the full Monte Carlo simulation of extensive air showers[25] and of the RPC array [26]. The excess significance measured in the $25^\circ < l < 100^\circ$, $|b| < 5^\circ$ region is 6.9 s.d.. The right plot in Fig 1 shows the Galactic latitude profile for the region $25^\circ < l < 100^\circ$. The line in the plots shows the flux at 600 GeV provided by the standard Fermi-LAT model for the diffuse Galactic emission $gal\_2yearp7v6\_v0.fits$ (hereafter Fermi-DGE) [2]. This is the first time

[1] http://tevcat.uchicago.edu

[2] http://fermi.gsfc.nasa.gov/ssc/data/access/lat/BackgroundModels.html

that a ground-based measurement of diffuse gamma-rays overlaps the direct ones. They are in fair agreement in the region $25^\circ < l < 100^\circ$, mostly in the range $40^\circ < l < 90^\circ$. The maximum deviations $\leq$2.5 s.d. are observed at three values outside this interval. In addition to statistical fluctuations, systematic uncertainties related to the background evaluation, imperfect modeling of the Galactic diffuse emission and other effects, for instance, an energy-dependent diffuse flux from unresolved sources, can contribute to this discrepancy. In the following sections, the spectral analyses concerning two selected subregions, $40^\circ < l < 100^\circ$ and $65^\circ < l < 85^\circ$, and the upper limit to the diffuse flux in the outer Galaxy are reported and discussed.

4.1 The Galaxy Region $25^\circ < l < 100^\circ$, $|b| < 5^\circ$

The energy spectrum is shown in the left plot of Fig 2. The spectral analysis uses the number of excess events measured in each N_{pad} group[27]. A differential spectral index -2.80 ± 0.26 is obtained. The corresponding median energies in the three N_{pad} intervals are 390 GeV, 750 GeV and 1.64 TeV, with an uncertainty of about 30%. Upper limits from Whipple, HEGRA and Tibet ASγ experiments are also shown[28][29][30]. The solid line represents the expectation according to the Fermi-DGE model extended to TeV energies with a spectral index -2.6 shown by the dashed line.

It is difficult to estimate the uncertainty of the model, which is in the range from 15% to 30% according to [31] [32]. Two main systematic uncertainties affect the ARGO-YBJ flux estimate, one on the background and the other on the absolute scale energy. Minor contributions come from the uncertainty on the residual contamination of the masked sources, from the uncertainty on the detector efficiency and on the effective area. The resulting total systematic error is $\sim$27%[33]. The estimated ARGO-YBJ flux at 1 TeV is $(6.0 \pm 1.3) \times 10^{-10}$ TeV^{-1} cm^{-2} s^{-1} sr^{-1}, 13% lower than the prediction based on the Fermi-DGE extrapolation. Taking into account the whole uncertainties, we deem the ARGO-YBJ data set consistent with the model predictions. It is worth noting that part of the detected signal could originate in faint sources that are unresolved. A treatment of these unresolved sources is discussed in[33], pointing out that while the main contribution from discrete sources has been removed, a residual contribution from unresolved sources could still affect the measured fluxes.

4.2 The Galaxy Region $40^\circ < l < 100^\circ$, $b < 5^\circ$

An excess with a statistical significance 6.1s.d. is observed in this region. The energy spectrum is shown in the right plot of Fig 2. A differential spectral index -2.90 ± 0.31 is obtained with a predicted flux at 1 TeV of $(5.2 \pm 1.5) \times 10^{-10}$ TeV^{-1} cm^{-2} s^{-1} sr^{-1}. The median energies in the three N_{pad} intervals are 350 GeV, 680 GeV and 1.47 TeV, with uncertainties of about 30%. The fluxes measured by ARGO-YBJ below 1 TeV are $\sim$20% larger than what expected by the Fermi-DGE model, however consistent within the experimental uncertainties.

Milagro made the first measurement of diffuse TeV gamma-rays from this region, showing a "TeV excess" anomaly. The differential flux at 3.5 TeV is reported in the right plot of Fig. 2 (triangle)[10]. This flux is only 34% greater than the value expected from the Fermi-DGE extrapolation, therefore within the experimental uncertainties. Moreover, the Milagro result does not take into account the contributions from sources such as the Cygnus cocoon, TeV J2032+4130, VER

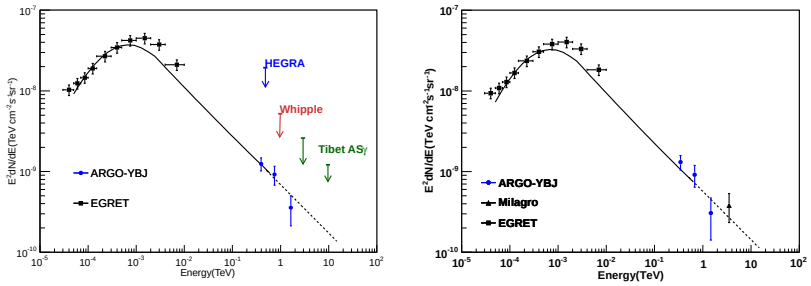

Figure 2: left: The energy spectrum of the diffuse gamma-rays in the Galactic region $25^\circ < l < 100^\circ$, $|b| < 5^\circ$ (dots). right: The energy spectrum of the diffuse gamma-rays in the Galactic region $40^\circ < l < 100^\circ$, $|b| < 5^\circ$ (dots).The solid line shows the flux in the same region according to the Fermi-DGE model. The short-dashed line represents its extension following a power law with spectral index -2.6. The EGRET results (squares) in the same Galactic region are also shown. The upper limits quoted by HEGRA (99% C.L., $38^\circ < l < 43^\circ$, $|b| < 2^\circ$), Whipple (99.9% C.L., $38.5^\circ < l < 41.5^\circ$, $|b| < 2^\circ$), and Tibet AS ęÃ (99%C.L., $20^\circ < l < 55^\circ$, $|b| < 2^\circ$) are also shown.

J2019+407 and VER J2016+372. Taking into account these corrections, we can conclude that the ARGO-YBJ and Milagro data are in fair agreement with the Fermi-DGE predictions, ruling out the evidence of any "TeV excess".

4.3 The Cygnus Region

An excess with statistical significance 6.7s.d. is found in the Galactic region $65^\circ < l < 85^\circ$, $|b| < 5^\circ$. After masking the discrete sources and the Cygnus cocoon and subtracting the residual contributions, an excess of 4.1s.d. is left. The spectral energy distribution is shown in the left plot of Fig 3. A differential spectral index -2.65 ± 0.44 is obtained with an estimated flux at 1 TeV of $(6.2 \pm 1.8) \times 10^{-10}$ TeV^{-1} cm^{-2} s^{-1} sr^{-1}, resulting about 10% lower than the Fermi-DGE extrapolation. The median energies in the three N_{pad} intervals are 440 GeV, 780 GeV and 1.73 TeV, with uncertainties of about 40%. Milagro measured the flux in the region $65^\circ < l < 85^\circ$, $|b| < 2^\circ$ at a median energy of 15 TeV that is shown in fig 3 by a filled triangle[11]. The Milagro flux is about 75% higher than the extrapolation of the Fermi template. One possible explanation of this discrepancy is that the contribution of all the discrete gamma-ray sources was not completely removed from the Milagro data.

An alternative explanation could be considered. Indeed, adding the data from the regions $25^\circ < l < 65^\circ$ and $85^\circ < l < 100^\circ$, we found an excess of 5.6 s.d with an index -2.89±0.33 and a flux at 1 TeV of $(6.0 \pm 1.7) \times 10^{-10}$ TeV^{-1} cm^{-2} s^{-1} sr^{-1}. Thus there is an indication that the spectrum of the diffuse emission in the Cygnus region could be harder than that in the complementary part of the $25^\circ < l < 100^\circ$ interval. The Cygnus region could contain a mixture of ordinary background cosmic rays and young cosmic rays with a harder spectrum not yet steepened by diffusion. The superposition of these two components may produce concave spectra at TeV energies[34] accounting for the Milagro result.

4.4 Outer Galaxy

No excess has been measured in the outer Galaxy region $130^\circ < l < 200^\circ$, $|b| < 5^\circ$, after

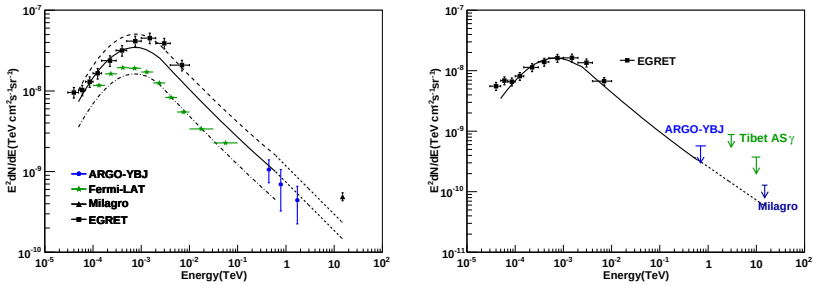

Figure 3: left: The energy spectrum of the diffuse gamma-rays in the Galactic region $65^\circ < l < 85^\circ$, $|b| < 5^\circ$. The solid line shows the flux according to the Fermi-DGE model, while the short-dashed one represents its extension following a power law with spectral index -2.6. The EGRET results (squares) are also shown. The Milagro result (triangle) is for the Galactic region $65^\circ < l < 85^\circ$, $|b| < 2^\circ$. The long-dashed line and its short-dashed extension represent the flux in this region according to the Fermi-DGE model. The energy distribution of gamma-ray emission measured by Fermi-LAT in the Galactic region $72^\circ < l < 88^\circ$, $|b| < 15^\circ$ is also reported (stars). The flux expected from the Fermi-DGE model is shown as a dot-dashed line. right: The 99% C.L. upper limit at a median energy of 700 GeV as obtained by ARGO-YBJ for the Galactic region $130^\circ < l < 200^\circ$, $|b| < 5^\circ$. The solid line shows the flux according to the Fermi-DGE model, while the short-dashed line represents its extension following a power law with spectral index -2.6. The EGRET results (squares) are also shown. The upper limit from Milagro (95% C.L., $136^\circ < l < 216^\circ$, $|b| < 2^\circ$) and those from Tibet ASgamma (99% C.L., $140^\circ < l < 225^\circ$, $|b| < 2^\circ$) are also reported.

masking the Crab Nebula. Assuming a spectral index -2.7 the median energy of all the events with $N_{pad} > 20$ is 700 GeV. The corresponding upper limit at 99% confidence level (C.L.) is 5.7×10^{-10} TeV^{-1} cm^{-2} s^{-1} sr^{-1} and is shown in Fig.3, where the limits obtained at higher energies by the Tibet ASγ (3 and 10 TeV) and Milagro (15 TeV) experiments are also reported. The Fermi-DGE flux and its extrapolation are shown for comparison. The ARGO-YBJ upper limit is compatible with the Fermi model, providing an useful constraint to the Galactic diffuse emission around 1 TeV.

5. Summary and conclusions

More than five years of ARGO-YBJ data have been used to study the diffuse gamma-rays from the Galactic plane. A spectral analysis of the data in the region $25^\circ < l < 100^\circ$, $|b| < 5^\circ$ has been carried out, showing an energy spectrum softer than that of the Fermi-DGE model, however consistent within 1 s.d.. On the other hand, the TeV flux averaged over the Cygnus region $65^\circ < l < 85^\circ$ shows a marginal evidence of a harder spectrum, indicating the possible presence of young cosmic rays coming from a nearby source. Only an upper limit has been set to the diffuse emission in the outer Galaxy region $130^\circ < l < 200^\circ$, $|b| < 5^\circ$, however compatible with the extrapolation of the Fermi-DGE model.

References

[1] Zhang, J., et al. 2010, ApJ, 720, 9

[2] Kniffen, D. A., & Fichtel, C. E. 1981, ApJ, 250, 389

[3] Strong, A. W., et al. 1987, A&A Suppl. Ser., 67, 283

[4] Hunter, S. D., et al. 1997, ApJ, 481, 205

[5] Strong, A. W. 2011, Proc. of the 12th ICATPP Conference, arXiv:1101.1381

[6] Abdo, A. A., et al. 2009a, Phys. Rev. Lett., 103, 251101

[7] Ackermann, M. et. al. 2012a, ApJ, 750, 3

[8] Abramowski, A., et al. 2014, Phys. Rev. D, 90, 122007

[9] Aharonian, F. A. et al. 2006a, Nature, 439, 695

[10] Atkins, R.W., et al. 2005, Phys. Rev. Lett., 95, 251103

[11] Abdo, A. A., et al. 2008, ApJ, 688, 1078

[12] Prodanović, T., Fields, B. D. & Beacom, J.F., 2007, Astropart. Phys., 27, 10

[13] Ackermann, M., Ajello, M., Allafort, A., et al. 2011, Science, 334, 1103

[14] Bartoli, B., et al. 2014a, ApJ, 790, 152

[15] Bartoli, B., et al. 2012a, Phys. Rev. D, 85, 092005

[16] He, H. H., Bernardini, P., Calabrese Melcarne, A. K., & Chen, S. Z. 2007, Astropart. Phys., 27, 528

[17] Aielli, G., et al. 2006, Nucl. Instrum. Meth. A, 562, 92

[18] Aielli, G., et al. 2009a, Astropart. Phys., 30, 287

[19] Aielli, G., et al. 2009b, Nucl. Instrum. Meth. A, 608, 246

[20] Bartoli, B., et al. 2011a, ApJ, 734, 110

[21] Bartoli, B., et al. 2011b, Phys. Rev. D, 84, 022003

[22] Bartoli, B., et al. 2013, ApJ, 779, 27

[23] Bartoli, B., et al. 2015, ApJ, 798, 119

[24] Fleysher, R., et al. 2004, ApJ, 603, 355

[25] Heck, D., et al. 1998, Report FZKA 6019

[26] Guo, Y.Q., et al. 2010, Chin. Phys. C, 34, 555

[27] Aielli, G., et al. 2010, ApJ, 714, L208

[28] LeBohec, S., Bond, I. H., Bradbury, S. M. et al. 2000, ApJ, 539, 209

[29] Aharonian, F. A. et al. 2001, A&A 375, 1008

[30] Amenomori, M., et al. 2006, Advances in Space Research, 37, 1932

[31] Macias, O. & Gordon, C. 2014, Phys. Rev. D, 89, 063515

[32] Ackermann, M. et. al. 2012c, ApJ Suppl. Ser., 203, 4

[33] Bartoli, B., et al. 2015, ApJ, 806, 20

[34] Gabici, S., Aharonian, F. A., & Casanova, S. 2009, MNRAS, 396, 1629